Arch. Metall. Mater. **69** (2024), 2, 541-544

DOI: https://doi.org/10.24425/amm.2024.149781

N.S. SUKIMAN[1], M.F. ZAVAWI[1], N. RAHMAT[1*], M.M. AL-BAKRI ABDULLAH[2]

EFFECT OF ANNEALING TEMPERATURE ON THERMAL BEHAVIOUR AND CRYSTALLINITY OF ZINC OXIDE SUPPORTED MAGNESIUM ALUMINATE ($ZnO/MgAl_2O_4$) VIA GREEN SYNTHESIS ONE POT FUSION

Zinc oxide-supported magnesium aluminate ($ZnO/MgAl_2O_4$) was synthesized by the one-pot fusion method, consuming magnesium nitrate, aluminum nitrate, and citric acid as starting precursors. The samples prepared were annealed at temperatures ranging from 700 to 900°C to study the influence of annealing temperature on thermal behaviour and crystalline properties. The thermal behaviour of $ZnO/MgAl_2O_4$ was characterized by thermogravimetric analysis (TGA), while the structural properties and crystalline phase of $ZnO/MgAl_2O_4$ were analysed by X-ray diffraction (XRD). The TGA results show that there were three stages of decomposition in the sample. The first stage indicates the removal of water content from the sample; the second stage indicates the decomposition of citric acid; and the third stage represents the crystallization phase formation at a temperature range of 800-950°C. The percentage of citric acid decomposition increases with increasing annealing temperatures up to 800°C. However, the decomposition rate gradually reduces at annealing temperatures between 850 and 900°C. XRD analysis results suggest that microstructured $ZnO/MgAl_2O_4$ with high crystallinity can be obtained at the highest annealing temperature. It can be concluded that the result of thermal behaviour represented by the decomposition stage is corroborated with structural and crystalline properties at increasing annealing temperatures.

Keywords: Magnesium Aluminate; One pot Fusion; Crystallinity; Thermal Behaviour; Green Synthesis

1. Introduction

Zinc oxide has garnered attention due to its unique combination of superior physical, chemical, biological, electrical, optical, long-term environmental stability, bio compatibility, low cost, and non-toxicity. It is a type of metal oxide with chemical formula of ZnO with white inorganic powder [1], inflammable and insoluble in water [2]. Photoelectric devices may use ZnO due to its wide band energy of 3.8 eV [3]. It can be used in catalysis to change organic reactants in chemical processes with excellent selectivity and efficiency due to its low retention time [4], less toxic [5], easy to dispose and recycle, environmentally friendly and cost efficient [1]. The rubber and textile industries employ zinc oxide powder as an ingredient due to its antibacterial, anti-fungal, fungicidal, and antimicrobial qualities. ZnO is usually used with PES to increase functional textile mechanical characteristics [6]. Due to its UV-absorbing properties, ZnO is also employed in pharmaceutical and cosmetic products like sunscreen [7].

There are numerous methods for synthesizing ZnO. Metallurgical process [8], controlled precipitation [9], sol gel process [10] and mechanochemical process [11] were conventionally used to synthesize ZnO. In a metallurgical process, ZnO was produced by heating or roasting zinc mineral residues or ore. Sol gel is another popular synthesis method that involves three main steps: the refluxing and boiling of zinc precursor, the formation of zinc clusters, and the formation of ZnO crystals at room temperature. Mixing zinc nitrate and zinc sulphate is required for the preparation of ZnO by precipitation. The mixture reactant is dissolved in 10 pH sodium hydroxide. The mixture is then sintered at a high temperature to produce ZnO nanoparticle powder. Previously, a sophisticated biological synthesis was utilized to synthesize ZnO from rambutan peel extract. Due to the biodegradable properties acquired from this synthesis [12], this method is sustainable and environmentally friendly.

Due to its stability, resistance to thermal shock, mechanical strength, and chemical inertness, magnesium aluminate ($MgAl_2O_4$) was extensively utilized in a previous study [13]. $MgAl_2O_4$ is useful for applications involving transparent windows, domes, and refractories [14]. It is an appropriate catalyst and support due to its thermal stability and low acidity [9], possesses porous structure and active centre for acidity or basicity [13,15]. In addition, $MgAl_2O_4$ is utilized in photoca-

[1] UNIVERSITI TEKNOLOGI MARA, SCHOOL OF CHEMICAL ENGINEERING, COLLEGE OF ENGINEERING, 40450 SHAH ALAM, SELANGOR, MALAYSIA
[2] UNIVERSITI MALAYSIA PERLIS, CENTRE OF EXCELLENCE GEOPOLYMER & GREEN TECHNOLOGY, 01000 KANGAR, PERLIS, MALAYSIA

* Coressponding author: norhasyimi@uitm.edu.my

talysis, ammonia synthesis, and methane dry reforming [15]. $MgAl_2O_4$ can be synthesized by sol-gel, co-precipitation, spray drying, spray pyrolysis and freeze drying [13]. In a sol-gel experiment, magnesium nitrate hexahydrate, $Mg(NO_3)_2 \cdot 6H_2O$ and aluminium tri-sec-butoxide $Al(OCH(CH_3)C_2H_5)_3$ are used as pre-cursors in an acidic medium at 80°C leading to the formation of magnesium aluminate, $MgAl_2O_4$ at 300°C. In another sol-gel study $MgAl_2O_4$ was formed at 700°C using $Mg(NO_3)_2$ and $C_6H_{14}O_3$ were used as precursors in citric acid [16]. $MgAl_2O_4$ can also be produced through the freeze-drying of the alkoxide precursor, $C_2H_6MgO_2$ and alumina sol in methanol. $MgAl_2O_4$ synthesized by co-precipitation is at temperatures between 700 to 900°C using ammonium dawsonite hydrate ($NH_4Al(OH)_2CO_3 \cdot H_2O$) and hydrotalcite ($Mg_6Al_2(CO_3)(OH)16 \cdot 4H_2O$) as precursors.

Using sol gel synthesis and wet precipitation with chemical or colloidal material, ZnO-supported $MgAl_2O_4$ formed an integrated network [17]. Colloid, a nanoparticle system disseminated in a solvent, is formed through the hydrolysis and poly-condensation of metal alkoxides and chlorides. In order to complete the protracted forming and densification procedure, an expensive chemical is required. In this investigation, $ZnO/MgAl_2O_4$ is produced using one-pot fusion green chemistry. In this one-step, dry procedure, Zn^{2+}, Al^{3+}, Mg^{2+}, and citric acid are used as precursors. Acid citric corrects the coordination of surfactants and inhibits precipitation.

2. Materials and methods

2.1. Chemicals

In this experiment, 0.1 mol magnesium nitrate hexahydrate ($Mg(NO_3)_3CH_2 \cdot 6H_2O$), 0.2 mol of aluminium nitrate hexahydrate ($Al(NO_3)_3 \cdot 9H_2O$) and 15.15 g zinc nitrate hexahydrate ($Zn(NO_3)2 \cdot 6H_2O$) were used as metal precursors and 0.3 mol citric acid ($HOC(COOH)(CH_2COOH)_2$) as surfactant material. All chemicals were acquired from Sigma Aldrich.

2.2. $ZnO/MgAl_2O_4$ synthesis

The amount of 0.1 mol $Mg(NO_3)_3CH_2 \cdot 6H_2O$, 0.2 mol ($Al(NO_3)_3 \cdot 9H_2O$), 0.3 mol ($HOC(COOH)(CH_2COOH)_2$) and 15.15g ($Zn(NO_3)2 \cdot 6H_2O$) were mixed and pulverized in a mortar for 1 hour. The mixture was pulverized until yogurt-paste like was formed. The pulverized sample was then transferred into a ceramic crucible and annealed at different temperatures from 700 to 900°C for 5 hours in a furnace.

2.3. Characterization of $ZnO/MgAl_2O_4$

The sample was characterised using X-ray diffraction model PANALYTICAL(Aeres) with Cu Kα radiation at 2θ from 5° to 70°. The scanning step used was 0.03 and scanning speed of 4° min^{-1}. The crystallite size of $ZnO/MgAl_2O_4$ was calculated using Scherrer's equation:

$$D_{xrd} = \frac{\kappa\lambda}{\beta \cos\theta}$$

Whereby D_{xrd} is crystallite size, κ is 0.9, β is full width half maximum (FWHM) in radian at strongest peak which is (1 0 1), (1 0 0) and (4 4 0). λ is wavelength at 1.5406Å and θ is the Bragg angle in degree.

Thermogravimetric analysis (TGA) method is a technique to measure the changes in the mass of material as the temperature changes [18]. The changes of mass due to the decomposition/degradation, vaporization, sublimation, reduction reactions and adsorption processes occur during the temperature changes. In this study, thermogravimetric analysis (TGA) was the method used to study the thermal behaviour of $ZnO/MgAl_2O_4$ samples using Mettler Toledo Gas STAR System, model TGA HT equipment in atmospheric air at a heating rate of 10° min^{-1} and an air flow rate of 20 ml min^{-1} from room temperature to 900°C.

3. Results and discussion

3.1. X-ray diffraction analysis

The XRD peak analysis of $ZnO/MgAl_2O_4$ for different annealing temperatures of 700 to 900°C is shown in Fig. 1. At different annealing temperatures, the XRD peak shows different degrees of intensity. Peaks at diffraction planes of (1 0 0), (3 1 1), (1 0 1), (4 4 0), and (5 3 1) indicate respective 2θ values of 31°, 36.5°, 38.2°, 59.3° and 64.6°. All peaks represent the face centred cubic of crystalline structure of $ZnO/MgAl_2O_4$ formed during annealing process. The strong peak of ZnO is

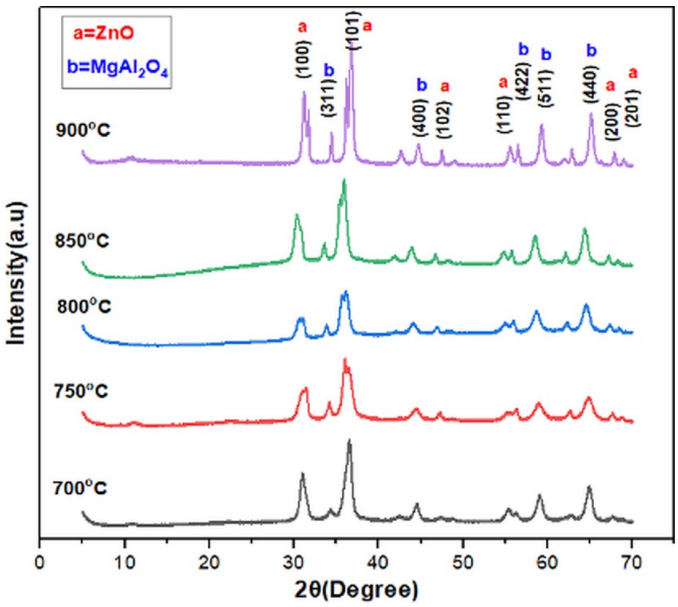

Fig. 1. The XRD pattern of ZnO-$MgAl_2O_4$ sample at different annealing temperature

significant at diffraction planes of (1 0 0), (1 0 1) and (1 1 0) at 2θ degree of 31°, 38.2° and 55.2°. $MgAl_2O_4$ displays strong peak attributed at 2θ of 36.5°, 59.3° and 64.6° which correspond to diffraction planes of (3 1 1), (5 1 1) and (4 4 0). The peak intensity shows an increase as the annealing temperature elevates to higher degree. This can be attributed to the high degree of $ZnO/MgAl_2O_4$ crystallinity as annealing temperature increases. (The magnesium aluminate has JCPD NO. 00-035-0965 and the zinc oxide magnesium aluminate has JCPD NO. 00-048-1023).

The average of crystallite size of particles at different annealing temperatures was calculated using Scherrer's equation. The three strongest peaks at diffraction planes of (1 0 1), (1 0 0) and (4 4 0) were chosen and the result was tabulated in TABLE 1. The crystallite size at different annealing temperatures for five hours significantly showed a gradual increase as the temperature elevated to 900°C. The crystallite size at diffraction planes of (1 0 1) increased from 15 nm at 700°C to 246 nm at 900°C. For diffraction planes at (1 0 0), the crystallite size was building up from 20 nm to 27 nm, while the diffraction planes of (4 4 0) showed size growth from 28 nm to 114 nm. This also concludes that the value of full-width half maximum (FWHM) decreased as the temperature increased. The lattice constant for the cubic phase of $ZnO/MgAl_2O_4$ at different temperatures ranged from 7.68Å to 8.38Å.

TABLE 1

Crystalline size of sample at different calcination temperature

Parameter	(1 0 1)	(1 0 0)	(4 4 0)
700°C	15 nm	20 nm	28 nm
750°C	23 nm	26 nm	34 nm
800°C	26 nm	26 nm	34 nm
850°C	36 nm	27 nm	41nm
900°C	246 nm	27 nm	114 nm

3.2. Thermogravimetric analysis

Fig. 2 displays the thermogravimetric analysis curve of ZnO-MgAl2O4 subjected to annealing at various temperatures ranging from 700 to 900°C. The heating procedure commenced at ambient temperature and was then elevated to 900°C, with a temperature ramp rate of 10°C per minute. Fig. 2 illustrates the comparison of the thermal gravimetric analysis (TGA) curve behaviour at various annealing temperatures. The data exhibits a negative correlation between weight loss and annealing temperature, suggesting a diminishing effect on weight reduction as the temperature of annealing rises. The thermogravimetric analysis (TGA) curve exhibits three distinct decomposition stages, each characterized by a unique weight loss. These weight loss values are presented in TABLE 2. In the case of the sample subjected to annealing at a temperature of 700°C, the thermal decomposition process can be divided into three distinct stages. The first stage occurs within the temperature range of 23 to 180°C, resulting in a weight loss of 2.67%. The second stage takes place from

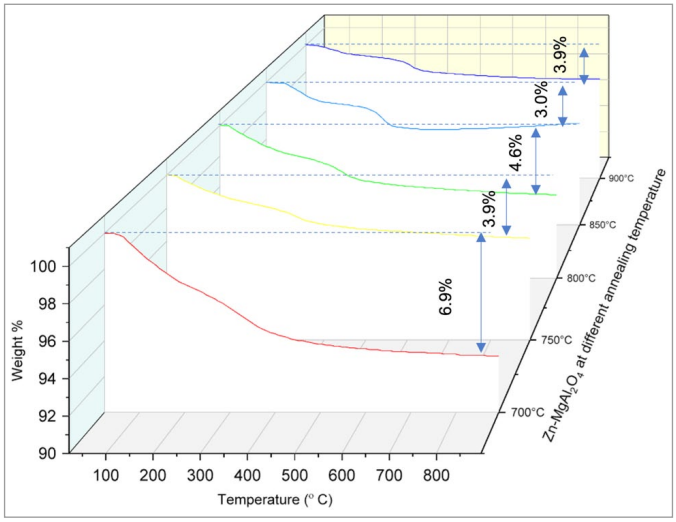

Fig. 2. The TGA curve behaviour for samples at different annealing temperature

200 to 600°C, leading to a weight loss of 3.68%. Finally, the third stage exhibits minimal weight loss, amounting to 0.36%, throughout the temperature range of 600 to 800°C. As the annealing temperature is elevated, the samples exhibit a declining pattern of weight loss during the initial and secondary stages of decomposition. However, the third stage of decomposition demonstrates a rising tendency in weight loss for samples subjected to temperatures ranging from 700 to 800°C. At a temperature of 850°C, there is a notable reduction in weight loss, which reduces to 0.15%. Additionally, the sample undergoes oxidation within the temperature range of 650 to 900°C.

TABLE 2

Weight loss at different stages of $ZnO\text{-}MgAl_2O_4$ for different annealing temperature

Calcination temperature	Decomposition stage	Weight loss %	Overall weight loss (%)
700°C	1st stage 2nd stage 3rd stage	2.67 3.68 0.36	6.9
750°C	1st stage 2nd stage 3rd stage	1.45 1.57 0.84	3.9
800°C	1st stage 2nd stage 3rd stage	1.84 1.81 0.91	4.6
850°C	1st stage 2nd stage 3rd stage	1.39 1.75 0.15	3.0
900°C	1st stage 2nd stage 3rd stage	0.99 1.05 0.5	3.9

Based on the findings depicted in Fig. 2 and TABLE 2, it can be inferred that the initial stage corresponds to the elimination of water, the subsequent stage corresponds to the decomposition of citric acid, and the last stage corresponds to the weight

loss associated with the crystallization phase of ZnO-$MgAl_2O_4$. The relationship between the third stage decomposition and the intensity peak and crystallite size obtained from XRD analysis is demonstrated in Fig. 1 and TABLE 1. A limited number of peak formations are discernible in the ZnO-$MgAl_2O_4$ sample during annealing at 800°C. These peaks are especially detected at diffraction planes measuring 36° and 48°. Notably, the intensity of these peaks increases as the annealing temperature is raised to 850 and 900°C. The observed phenomenon of diminishing weight loss and oxidation at the third stage of breakdown for samples subjected to temperatures of 800°C and above can potentially be elucidated by this explanation.

4. Conclusion

The synthesis of ZnO/$MgAl_2O_4$ microstructure was successfully accomplished by a one-pot fusion method. The thermal characteristics of the samples were examined using thermogravimetric analysis (TGA) and then compared with the results obtained from X-ray diffraction (XRD) analysis. The sample exhibited three distinct stages of disintegration. The initial stage involves the extraction of moisture from the specimen, the subsequent stage involves the breakdown of citric acid, and the last stage signifies the production of crystalline phases. The X-ray diffraction (XRD) analysis revealed data that supported the presence of a cubic crystal structure in the ZnO/$MgAl_2O_4$ composite. Based on the observed behaviour of the third decomposition stage, it can be inferred that there is a positive correlation between temperature and crystallite size.

Acknowledgement

Research grant FRGS/1/2018/TK05/UiTM/03/7 and 600-RMC/GPM LPHD 5/3 (077/2022) are gratefully acknowledged for supporting the present research study.

REFERENCES

[1] K.S.Siddiqi, et al., Properties of zinc oxide nanoparticles and their activity against microbes. Nanoscale Res Lett **13** (1), 141 (2018).

[2] A. Moezzi, et al., Zinc oxide particles: Synthesis, properties and applications. Chemical Engineering Journal **185-186**, 1 (2012).

[3] L. Saad, et al., Characterization of various zinc oxide catalysts and their activity in the dehydration-dehydrogenation of isobutanol. Journal of the Serbian Chemical Society **73** (10), 997 (2008).

[4] K.B. Baharudin, et al., Effect of calcination temperature on the physicochemical properties of zinc oxide nanoparticles synthesized by coprecipitation. Materials Research Express **5** (12) 125018 (2018).

[5] J.N. Hasnidawani, et al., Synthesis of ZnO nanostructures using sol-gel method. Procedia Chemistry **19**, 21, 1 (2016).

[6] M. Fiedot-Tobola, et al., Deposition of zinc oxide on different polymer textiles and their antibacterial properties. Materials (Basel) **11** (5), 707 (2018).

[7] T. Goto, et al., Morphological control of zinc oxide and application to cosmetics. International Journal of Nanotechnology **10** (1/2), 48 (2013).

[8] R. Škuta, et al., Utilization of metallurgical waste for the preparation of photocatalytically active composites based on ZnO–graphene oxide. Chemical Papers **75** (8), 3891 (2021).

[9] J.E. Rodriguez-Paez et al., Controlled precipitation methods: formation mechanism of ZnO nanoparticles. Journal of the European Ceramic Society (21), 925 (2001).

[10] K.A.Abdullah, et al., Synthesis of ZnO nanopowders by using sol-gel and studying their structural and electrical properties at different temperature. Energy Procedia **119**, 565 (2017).

[11] Z. Zhou, et al., ZnO nanospheres fabricated by mechanochemical method with photocatalytic properties. Catalysts **11** (5) (2021).

[12] A. Kolodziejczak-Radzimska, et al., Zinc oxide-from synthesis to application: A Review. Materials (Basel) **7** (4), 2833 (2014).

[13] I. Ganesh, A review on magnesium aluminate ($MgAl_2O_4$) spinel: synthesis, processing and applications. International Materials Reviews **58** (2), 63 (2013).

[14] R. Sarkar, Refractory applications of magnesium aluminate spinel. International Ceramic Review p. 11 (2010).

[15] S.A. Theofanidis, et al., Fe-containing magnesium aluminate support for stability and carbon control during methane reforming. ACS Catalysis **8** (7), 5983 (2018).

[16] P. Fu, et al., Thermal stability and microstructure characterization of $MgAl_2O_4$ nanoparticles synthesized by everse microemulsion method. Materials Research **16** (4), 844 (2013).

[17] P. Pathak, et al., Investigation of structural and optical properties of $Zn0_{67}Mg0_3Al_2O_4$:0.03Dy nanophosphor. Materials Today: Proceedings **47**, 6854 (2021).

[18] K. Slopiecka, et al., Thermogravimetric analysis and kinetic study of poplar wood pyrolysis. Applied Energy **97**, 491 (2012).